Catal Lett (2017) 147:1040–1050
DOI 10.1007/s10562-017-1997-5

Mesoporous MCM-48 Immobilized with Aminopropyltriethoxysilane: A Potential Catalyst for Transesterification of Triacetin

Mahuya Bandyopadhyay[1,2] · Nao Tsunoji[1] · Tsuneji Sano[1]

Received: 15 December 2016 / Accepted: 13 February 2017 / Published online: 28 February 2017

Abstract The ordered mesoporous silicas MCM-48, MCM-41, and SBA-15 were synthesized and functionalized with 3-aminopropyltriethoxysilane (APTES). The X-ray diffraction patterns before and after functionalization revealed no structural degradation during the process. FT-IR spectra of the materials clearly indicated the anchoring of the aminopropyl moiety with silanol groups. The amine concentrations were calculated using TG-DTA and CHN analysis. The amine-loaded materials were assessed as catalysts for the transesterification of triacetin with methanol. MCM-48-NH_2, in which the pores are interconnected in a three-dimensional manner, exhibited superior catalytic activity to one- dimensional MCM41-NH_2 and SBA-15-NH_2, even with lower concentrations of the amine group.

Graphical Abstract

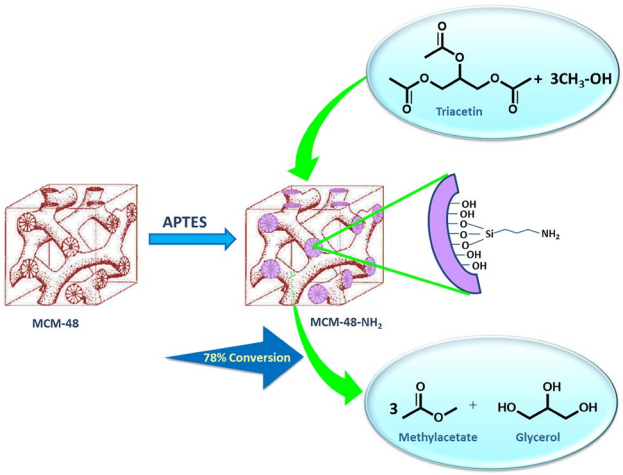

Keywords Mesoporous materials · Functionalization · MCM-48 · Transesterification · Triacetin

1 Introduction

The increasing global demand for energy has led to intense research activity into alternative energy sources. Bio-based resources are considered as a promising renewable alternative energy source to fossil fuels owing to the environmental hazards and lack of sustainability associated with the latter [1, 2]. However, the high viscosity of vegetable oil, one of the most common bio-based resources, prevents its direct use as a fuel for diesel engines. Modifications including dilution, pyrolysis, microemulsification, and, most successfully, transesterification, have been employed to overcome this problem. Consequently, the production of

Electronic supplementary material The online version of this article (doi:10.1007/s10562-017-1997-5) contains supplementary material, which is available to authorized users.

✉ Mahuya Bandyopadhyay
mouraji@hiroshima-u.ac.jp

✉ Nao Tsunoji
tnao7373@hiroshima-u.ac.jp

[1] Department of Applied Chemistry, Graduate School of Engineering, Hiroshima University, Higashi-Hirosima 739-8527, Japan

[2] Institute of Infrastructure, Technology, Research and Management, IITRAM, Maninagar, Ahmedabad, Gujarat, India

biodiesel from the transesterification of vegetable and animal fats using homogeneous base catalysts has increased drastically in recent years.

Natural fats and oils can be used for the production of a variety of bio-based products because they contain multiple reactive groups that can be modified to afford the desired products using an appropriate choice of reaction conditions and catalyst. Triglycerides, which are produced from plants and animal fats, are regarded as a prospective source for bio-fuel production because they have a composition similar to that of fossil fuels [3]. Methyl esters are produced by the transesterification of triglycerides with short chain alcohols such as methyl alcohol. However, the major challenge in this process is to convert the material into bio-fuels. To improve the economical aspect of these processes, the choice of catalyst is crucial. Homogeneous catalysts are ideal for liquid-phase reactions because they form uniform mixtures with the reactants, resulting in minimum mass-transfer limitations and high reaction rates. However, the use of homogeneous catalysts presents certain difficulties, including the disposal of toxic wastes, complicated catalyst recovery, and time- and energy-consuming separation of the desired products. These unfavorable aspects of the use of homogeneous catalysts have led to an increase in the use of solid heterogeneous catalysts for large-scale chemical reactions [4–6]. Alkali-earth-metal oxides [7], alkali–metal-doped alumina [8, 9], metal-loaded zeolites [10], hydrotalcites [11], enzymes [12], Amberlyst-15 [13], the Cs salt of $H_3PW_{12}O_{40}$ [13], and polyaniline sulfate [14] have been studied as heterogeneous catalysts for the transesterification of triglycerides.

The transesterification of triacetin on alkali–metal-modified nano-silicalite-1 has been recently reported [15]. In this study, the authors doped nano-silicalite-1 with different alkali metals, including Cs, Li, and K, and compared the catalytic activities of the resultant materials. Zeolites attract considerable attention as heterogeneous catalyst supports owing to their unique pore structure, high surface area, and high hydrothermal stability [16]. Lopez et al. [17] reported the comparison of a variety of solid catalysts and conventional liquid catalysts, such as NaOH and H_2SO_4, in the transesterification of triacetin as a model reaction for that of the larger triglycerides found in vegetable oils and fats. However, the use of zeolite-type catalysts for liquid-phase reactions involving biological feedstock where larger molecules are involved has met with limited success because these types of reactions require well-defined domains to minimize the formation of unwanted byproducts. This poor performance has led to extensive research into increasing the pore size of mesoporous materials while maintaining their high surface area. A major breakthrough in this research was the fabrication of MCM type mesoporous materials by the scientists of the Mobil Research and Development Company in 1992 [18]. Following appropriate functionalization, these types of mesoporous materials can serve as potential catalysts to increase the yield of, and selectivity for, the desired products. Several approaches have been proposed to impart specific properties to these materials for application in areas such as catalysis, chemical sensing, and adsorption [19–23].

The heterogenization of organic bases has been used to prepare catalysts that exhibit excellent performance in many reactions. Surface functionalization of mesoporous materials allows the introduction of catalytic groups to their internal pore surfaces through co-condensation or post-synthesis treatment [24]. MCM-41- and MCM-48-type materials contain a large number of –OH groups on their internal pore surfaces that can react to form hybrid materials. Surface modification by the formation of silanol linkages via condensation with silane-bearing moieties, particularly propyl chains, is the most commonly employed methodology [25–36]. Modification with silane-terminated aminopropyl chains, which imparts surface basicity to the mesoporous materials, has been particularly widely studied [37, 38]. Mesoporous materials particularly MCM-41, and SBA-15 has been widely explored in esterification reaction so far, but almost no report has been available for mesoporous MCM-48 materials employed in this reaction. Guerrero et al. has reported amine functionalized MCM-41 and SBA-15 as transesterification catalysts of glyceryl tributyrate with methanol [39].

MCM-48, a relatively unexploited mesoporous siliceous molecular sieve, has been investigated in the present work. Its interconnected three-dimensional pore structure was expected to provide a combination of catalytic activity and product selectivity superior to that available from other catalysts, including those based on more common mesoporous molecular sieves such as MCM-41 and SBA-15, in which the pores extend in only one direction. This limits the accessibility to active sites in these materials, restricting the level of functionalization, and extending diffusion distances for reactants and products. However, there remains the question of whether it is simply the accessibility of the active sites in functionalized MCM-48 that renders it more active, or whether the active sites on this support have higher catalytic activity, or indeed differ in any other way, from those of MCM-41 and SBA-15.

The objective of this study was to compare MCM-48 with MCM-41 and SBA-15 as siliceous catalyst support materials in terms of the concentration of the supported aminopropyl groups, and to relate these properties to the catalytic activities of the supported basic groups. The approach taken was to prepare the siliceous supports and then functionalize them with 3-aminopropyltriethoxysilane (APTES). The obtained hybrid materials were thoroughly characterized by means of X-ray powder diffraction (XRD),

N_2 adsorption, thermogravimetric and differential thermal analysis (TG-DTA), Fourier-transform infrared (FT-IR) spectroscopy, and solid-state MAS NMR.

A series of catalysts containing different concentrations of amine groups were synthesized, and these amine-functionalized mesoporous materials were then employed as catalysts for the transesterification of triacetin with methanol. Different reaction parameters were studied, and the reaction conditions were optimized. The results correlated well with the nature of the supports. Heterogeneity was also tested on the most effective catalyst to confirm the absence of any leaching of the active species from the support surface. The excellent results obtained for amine-functionalized MCM-48 as a catalyst for transesterification is the key finding of this work.

2 Experimental

2.1 Synthesis of MCM-48

In a typical procedure [40], cetyltrimethylammonium chloride (CTACl, >95%, TCI) was added to 1 M NaOH in a Teflon bottle. The appropriate amount of water was then added, and the mixture was stirred in a water bath at 50 °C until it became homogeneous, followed by the addition of tetraethoxysilane (TEOS, Wako). The final molar gel composition was 1.0 TEOS:0.7 CTACl:0.5 NaOH:64 H_2O. The obtained gel was poured into a Teflon-lined autoclave and kept at 90 °C for four days. The product was filtered off, washed thoroughly with water, and dried at room temperature. The surfactant inside the as-synthesized material was removed by calcination at 540 °C for 5 h.

2.2 Synthesis of MCM-41

Cetyltrimethylammonium bromide (CTMABr, >98%, TCI) was dissolved in a solution of NaOH (0.1 M) at 40 °C. After dissolution, TEOS was added to the mixture. The mixture was stirred for 2 h and poured into a Teflon bottle. The gel was kept at 100 °C for 24 h. The final molar gel composition was 1.0 TEOS:0.12 CTABr:0.23 NaOH:130 H_2O. The product was filtered off, washed thoroughly with water, and dried at room temperature. The surfactant template was removed by calcination at 540 °C for 5 h [41].

2.3 Synthesis of SBA-15

The poly(ethylene glycol)-block-poly(propylene glycol)-block-poly(ethylene glycol)-block copolymer (Pluronic 123, Aldrich) was used as a template. First, the solid copolymer was mixed with 2 M HCl and stirred for 3 h until a clear solution was obtained. The solution was then heated at 40 °C. Finally, TEOS was added, and the mixture was stirred at room temperature for 20 h. The solution was then poured into a Teflon-lined autoclave and aged at 90 °C for 24 h. The final molar gel composition was 1.0 TEOS:0.017 Pluronic123:6.1 HCl:165 H_2O. After hydrothermal treatment for 24 h the product was filtered off, washed thoroughly with water, and dried at room temperature. The obtained material was calcined in air at 540 °C for 5 h [42].

2.4 Functionalization of Mesoporous Silica

In each case, 1 g of the mesoporous silica was dried under vacuum at 70 °C for 4 h. After the pre-treatment, the mesoporous silica was dispersed in 50 mL of toluene and an excess amount (1:1 weight ratio) of APTES (>99%, Aldrich) was added. The mixture was vigorously stirred under reflux for 12 h. The solid product was then collected by filtration, washed thoroughly with toluene, and air dried [43]. A series of mesoporous silicas with different aminopropyl concentrations were prepared.

2.5 Catalyst Characterization

The as-synthesized, calcined, and functionalized materials were characterized using powder XRD using a Bruker AXS D8 Advance diffractometer with graphite monochromatized CuKα radiation at 40 kV and 30 mA. Scanning electron microscopy (SEM) images were recorded using a Hitachi-S-4800 SEM coupled with an energy-dispersive X-ray (EDX) analyzer. ^{29}Si magic-angle spinning (MAS) NMR spectra were recorded at 119.18 MHz on a Varian 600PS solid NMR spectrometer using a 6 mm diameter zirconia rotor spinning at 4 kHz. The spectra were acquired using 6.2 μs pulses, a 100 s recycle delay, and 1000 scans. 3-(Trimethylsilyl) propionic-2,2,3,3-d_4 acid sodium salt was used as a chemical shift reference. ^{1}H–^{13}C cross-polarized (CP) MAS NMR spectra were measured with a spinning frequency of 4 kHz, a 90° pulse length of 5.6 μs, and a cycle delay time of 5 s. The ^{13}C chemical shifts were referenced to hexamethylbenzene. Thermal analyses were performed using an SII 7300 TG-DTA instrument (Seiko Instruments). A sample of 3–4 mg was heated in a flow of air (50 mL min^{-1}) at a heating rate of 10 °C min^{-1} from room temperature to 700 °C. N_2 adsorption/desorption measurements were carried out at −196 °C using a conventional volumetric apparatus (BELSORP-max, Bel Japan). The calcined samples were degassed at 400 °C for 16 h under N_2 flow prior to analysis. The functionalized samples were heated at 200 °C. CHN analysis was performed using a Perkin-Elmer 2400 11 CHN analyzer at the Natural Science Centre for Basic Research and Development (N-BARD), Hiroshima University. IR spectra were recorded at room

temperature on an FT-IR spectrometer (NICOLET 6700) at a resolution of 4 cm^{-1}.

2.6 Catalytic Activity Measurement

The amine-modified mesoporous silica sample (10 mg) was activated at 70 °C for 1 h. Transesterification of triacetin (>98%, TCI) with methanol (>99.8%, KANTO CHEMICAL) was performed in a glass tube fitted with a screw cap. For the reaction, 3 g of triglyceride triacetin was mixed with 6.52 g methanol (i.e., at a methanol: triacetin molar ratio of 16:1). The reaction was performed at 65 °C for 270 min under stirring. After completion of the reaction, the filtrate was separated from the catalyst and 0.0166 g (100:1 mmol with respect to triacetin) of solid naphthalene was used as an internal standard. Samples were analyzed using a Shimadzu-14B gas chromatographer (GC) equipped with a flame ionization detector and a Stabilwax column using Ar as a carrier gas to determine the conversion of triacetin and the product yield.

3 Results and Discussion

3.1 Catalyst Characterization

The XRD patterns of as-synthesized, calcined, and amine-modified MCM-48, MCM-41, and SBA-15 are shown in Fig. 1. The siliceous MCM-48 sample shows characteristic reflections from the 211, 220, 420, and 332 planes. The patterns imply that all the materials are well-ordered, well-resolved, and periodic, indicating good long-range order. For the calcined sample, a decrease in the unit cell volume caused by the condensation of silanol groups is observed (i.e., in the XRD pattern of MCM-48), which is indicated by the shift of the 211 peak from $2\theta = 2.20°$ to $2\theta = 2.70°$. All reflections exhibit increased intensity due to increased diffraction contrast between the channel pores and walls upon removal of the surfactant template [40]. The peak intensities decrease upon modification with APTES in all cases. This decrease in peak intensity is caused by the grafting of aminopropyl groups in the mesoporous moiety. Furthermore, the intensities of the peaks between $2\theta = 4.7°–5.3°$ (MCM-48-NH_2) and $2\theta = 3.87°–5.11°$ (MCM-41-NH_2) decrease significantly. In these types of mesoporous materials, the peak intensity characteristics depend on the scattering contrast between the pore walls and pore channels, and usually decrease with a decrease in scattering contrast upon anchoring of organic groups to the pore surfaces [44]. Thus, pore occupancy by the tethered organic groups is the most likely cause of the observed decrease in peak intensity, rather than any change in the mesostructure. Thus, the mesoporosity and homogeneity of all the support materials appear to be maintained.

The success of the post-synthetic grafting of organic moieties is also confirmed by TG-DTA. The initial weight loss of ~2% up to 500 K is mainly due to desorption of physically adsorbed water. The substantial weight loss from 600 to 900 K results from the decomposition of organic groups anchored in the mesoporous matrices. The amount of organic materials anchored via silanol groups was evaluated from the weight loss in this temperature range. This result is also confirmed by the occurrence of a sharp exothermic peak in the DTA curve at ca. 600 K for all the materials (see Fig. S1). The amine concentrations obtained from TG analysis of the different silica materials are listed in Table 1. CHN analysis was also done for most active catalysts and given in Table 1. The obtained values are constant with that from TG analysis. To gain a better understanding of the influence of the organic compound, we prepared several catalysts with different amine-loading amounts.

In order to further confirm the presence of amine groups anchored through the grafting process, FT-IR spectra of the materials before and after amine loading were compared, as shown in Fig. 2. All the bare materials exhibit broad peak at 3400 cm^{-1} owing to the O–H bond (data not shown) of the silanol group, and the peaks at 1070 and 795 cm^{-1} correspond to Si–O–Si stretching and bending vibrations, respectively [45]. The signal at 1516 cm^{-1} is attributed to NH_2 scissoring [46]. This peak is observed for all the mesoporous silicas. The C–N stretching vibration is usually observed in the wavelength range 1000–1200 cm^{-1}, but this peak cannot be resolved owing to overlap with the Si–O–Si

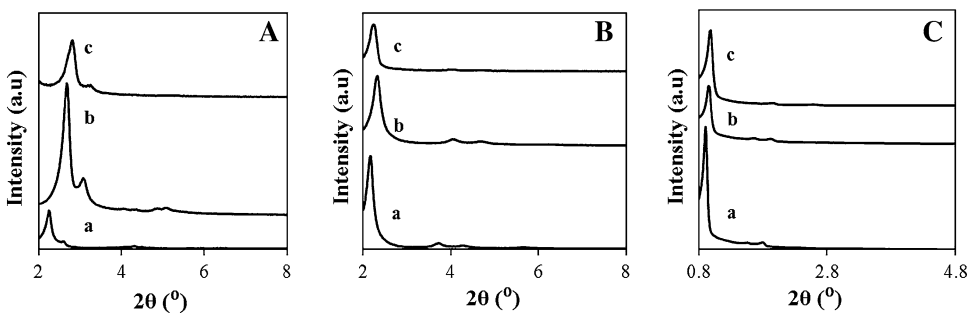

Fig. 1 Powder XRD patterns of *a* as-synthesized, *b* calcined, and *c* amine-loaded mesoporous silicas **A** MCM-48, **B** MCM-41, and **C** SBA-15

Table 1 Preparation and characteristics of various amine modified mesoporous materials

Catalyst	Amine concentration[a] (mmol g^{-1})	Amine concentration[b] (mmol g^{-1})	BET surface area[c] (m^2 g^{-1})	Pore volume[d] (cc g^{-1})	Pore diameter[d] (nm)
MCM-48	0	–	1351	1.1	2.34
MCM-48-NH_2 (1:1)	1.24	1.12	400	0.36	1.54
MCM-48-NH_2 (1:0.5)	1.05	1.01	385	0.35	1.55
MCM-48-NH_2 (1:0.025)	0.52	–	498	0.52	1.54
MCM-48-NH_2 (1:0.01)	0.43	–	460	0.56	1.54
MCM-48-NH_2 (1:0.005)	0.31	–	900	0.85	1.54
MCM-48-NH_2 (1:0.001)	0.17	–	861	0.55	2.08
MCM-41	0	–	1088	0.99	2.51
MCM-41-NH_2 (1:1)	1.31	1.25	690	0.31	1.83
MCM-41-NH_2 (1:0.025)	0.38	–	881	0.65	2.48
SBA-15	0	–	852	0.96	6.4
SBA-15-NH_2 (1:1)	1.36	1.78	282	0.39	5.34
SBA-15-NH_2 (1:0.025)	0.5	–	755	0.87	6.4

[a]Determined from thermogravimetric analysis (TG-DTA)

[b]Determined from CHN analysis

[c]Surface area determined by the BET method

[d]Determined by the BJH method

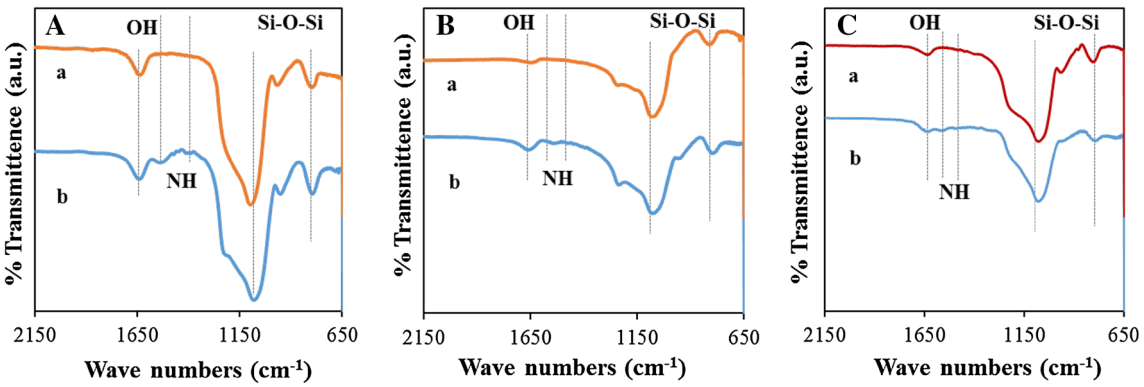

Fig. 2 FT-IR spectra of *a* calcined, and *b* amine-loaded mesoporous silicas **A** MCM-48, **B** MCM-41, and **C** SBA-15

band presented at 1050–1150 cm^{-1}. However, the peak for the modified silicas in this range is wider, suggesting a possible overlap of the peaks. Thus, the covalent grafting of APTES onto the mesoporous silica materials may be clearly established by comparing the spectra of the grafted and unloaded materials.

N_2 adsorption/desorption analysis of the pure and functionalized materials are shown in Fig. 3. The adsorption/desorption isotherm data are given only for the most active catalyst (Silica:APTES = 1:1), and the amine-modified materials are compared with pure unloaded mesoporous silica materials. The N_2 adsorption isotherms of the pure samples are of type IV with a sharp capillary condensation step between the partial pressures 0.1 and 0.8, which is characteristic of typical mesoporous materials with uniform pore-size distribution. The surface area and porosity data obtained from the adsorption branch are summarized in Table 1 (see Fig. S2). The surface area, pore volume, and pore diameter decrease with an increase in amine concentration. For MCM-48, the decrease is much more pronounced in the case of the bare and 1:1 Silica:APTES (*w*/*w*) material. However, the surface areas of the samples prepared with ratios of 1:1, 1:0.5, 1:0.025, and 1:0.01 are almost the same, and this is reflected in the catalytic activities of these catalysts, as discussed in Sect. 3.2. The pore diameter decreases from 2.34 to 1.54 nm, and this value is almost the same for all the MCM-48 samples prepared with different amine concentrations. However, in the cases of MCM-41 and SBA-15, there is also no significant change in pore diameter

upon decreasing the amine loading (1:0.025 silica: amine (*w*/*w*)). Furthermore, there is no significant change in the surface area. These two samples show significantly lower catalytic activity, which is in perfect agreement with the porosity data. The presence of the amine groups reduces the effective surface area, which is indicated by the decrease in the height of the capillary condensation step. The pore volume and pore diameter also decrease upon amine functionalization. This is expected, as the amine group is tethered to both the external and internal pore surfaces. The maximum reduction of pore diameter is observed for the amine modified MCM-48 materials, which is consistent with the catalytic activity results presented in Sect. 3.2.

The SEM images of the amine-loaded materials are shown in Fig. 4. The MCM-48-NH_2 particles present a uniformly spherical morphology with a particle size of ~250 nm. The MCM-41-NH_2 particles are disc shaped with a diameter of ~2.0 μm, whereas the SBA-15-NH_2 particles appear chain-like with lengths of ~1.5 μm. It is also confirmed that modification with the aminopropyl group does not alter the morphology of the samples.

Figure 5 shows TEM images of MCM-48-NH_2, MCM-41-NH_2, and SBA-15-NH_2. The periodic arrangement of

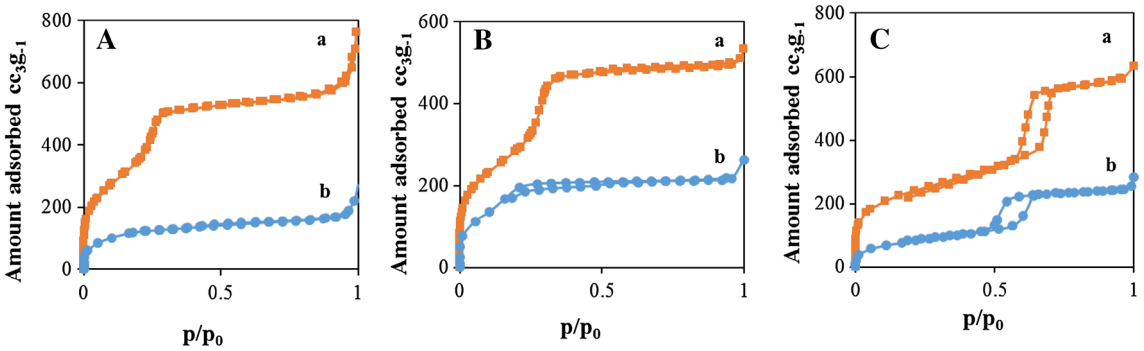

Fig. 3 N_2 adsorption/desorption isotherms of *a* calcined and *b* amine-loaded mesoporous silicas **A** MCM-48, **B** MCM-41, and **C** SBA-15

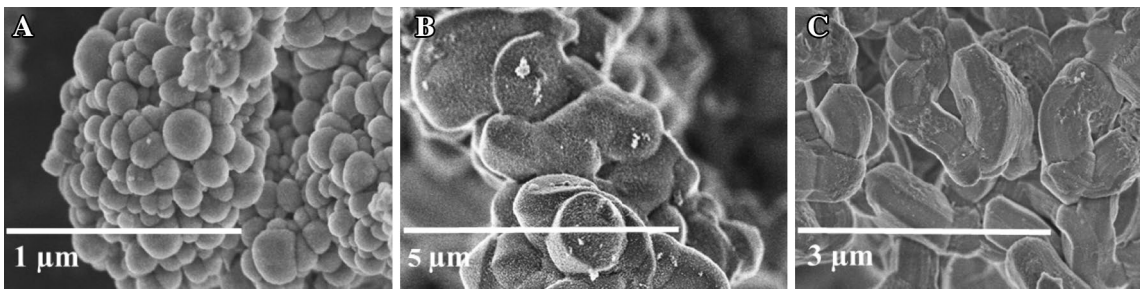

Fig. 4 SEM images of **A** MCM-48-NH_2, **B** MCM-41-NH_2, and **C** SBA-15-NH_2

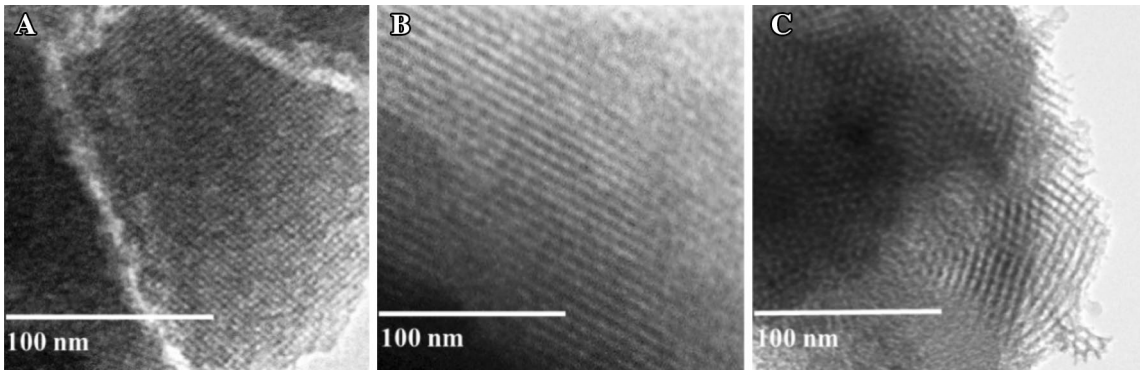

Fig. 5 TEM images of **A** MCM-48-NH_2, **B** MCM-41-NH_2, and **C** SBA-15-NH_2

walls and channels in the mesoporous materials leads to periodic imaging contrast in the TEM observation. The regular contrast variation in the image indicates the intact silicate framework. There is no sign of structure distortion upon amine grafting and subsequent prolonged washing and drying.

The ^{29}Si MAS NMR and ^{13}C CP MAS NMR spectra of the materials are given in Figs. 6 and 7, respectively. In the ^{29}Si MAS NMR spectra, the unloaded materials present signals due to **Si**$(OSi)_3(OH)$ (Q^3) and **Si**$(OSi)_4$ (Q^4) at −102 and −111 ppm, respectively. After amine loading, a broad signal at −60 to −70 ppm ascribed to C–Si$(OSi)_3$ (T^3) is clearly observed in all the mesoporous silica samples, indicating the successful silylation by amine functionalized groups. In the case of the ^{13}C CP MAS NMR spectra, resonances around δ = 10, 21, and 42 ppm, attributed to amine propyl groups, are observed. These spectra match well with the literature data [47], also confirming the presence of aminopropyl groups on the silica surface.

3.2 Catalytic Activity Test

3.2.1 Comparison of Various Catalysts

The catalytic activities of the materials in the transesterification of triacetin (the acetic acid triester of glycerol) with methanol was screened. The methanolysis of triacetin, which is the simplest triglyceride, has been studied here as a model reaction. As transesterification is an

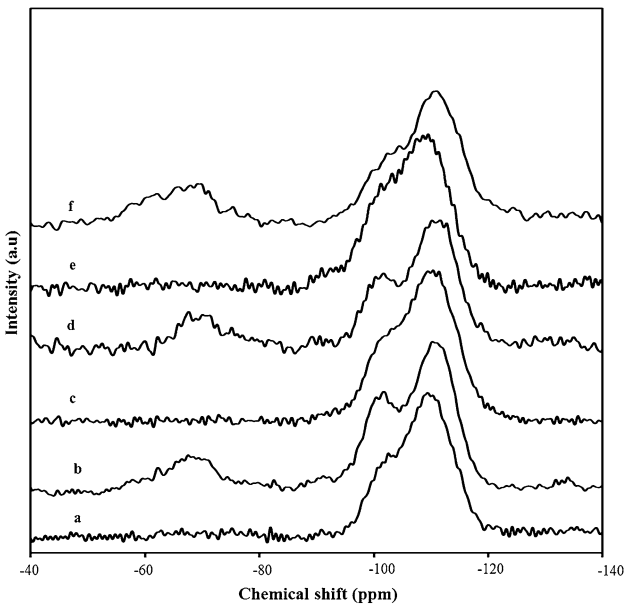

Fig. 6 ^{29}Si MAS NMR spectra of *a* MCM-41, *b* MCM-41-NH_2 (Silica:APTES = 1:1), *c* MCM-48, *d* MCM-48-NH_2 (Silica:APTES = 1:1), *e* SBA-15, and *f* SBA-15-NH_2 (Silica:APTES = 1:1)

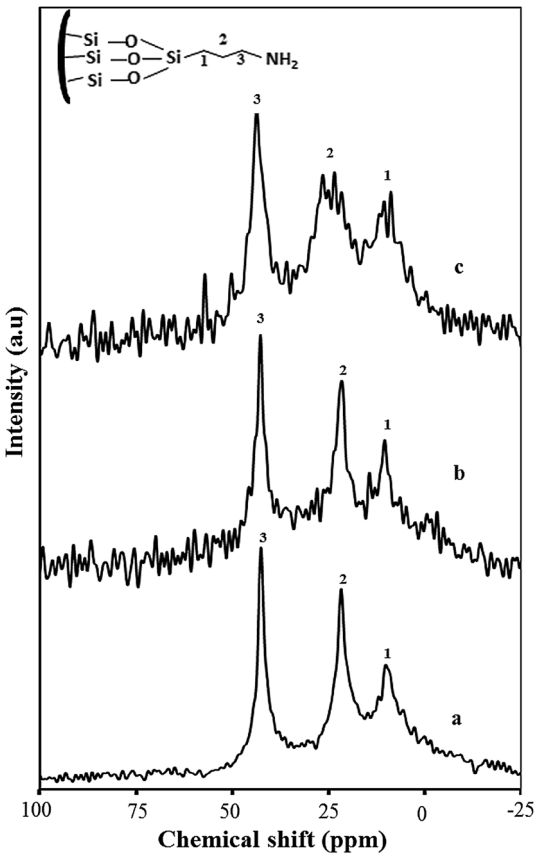

Fig. 7 ^{13}C CP MAS NMR spectra of *a* MCM-41-NH_2 (Silica:APTES = 1:1), *b* MCM-48-NH_2 (Silica:APTES = 1:1), and *c* SBA-15-NH_2 (Silica:APTES = 1:1)

equilibrium-controlled reaction, a higher methanol/triacetin molar ratio is necessary to shift the equilibrium to the product side and increase triglyceride conversion. Therefore, the catalytic reactions were performed at 65 °C for 4.5 h with methanol/triacetin molar ratio of 16. For all reactions, 10 mg of catalyst was used. The activities are expressed in terms of triacetion conversion, and the main desired product, methylacetate, was identified. The catalytic activity results for different silica materials are depicted in Fig. 8. Amine-loaded MCM-48 (Silica:APTES = 1:1) shows 78% triacetin conversion and a 52% methyl acetate yield, whereas MCM-41-NH_2 (Silica:APTES = 1:1) shows 34% triacetin conversion and 6% yield, and SBA-15-NH_2 (Silica:APTES = 1:1) shows 37% conversion and 5% yield.

3.2.2 Effect of Reaction Time

The detailed kinetics was investigated for all the catalysts, and the results are summarized in Fig. 9. The MCM-48-NH_2 (Silica:APTES = 1:1) catalyst exhibits excellent performance in this reaction, even at shorter reaction times. It can be concluded from the time

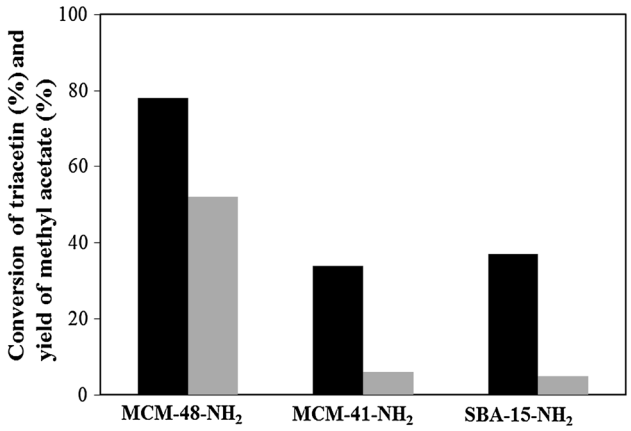

Fig. 8 Transesterification of triacetin with methyl alcohol over MCM-48-NH_2 (Silica:APTES = 1:1), MCM-41-NH_2 (Silica:APTES = 1:1), and SBA-15-NH_2 (Silica:APTES = 1:1) catalysts. *Black* represents conversion of triacetin and *grey* represents yield of methyl acetate. Reaction conditions: catalyst 0.01 g, temperature 65 °C, and time 4.5 h

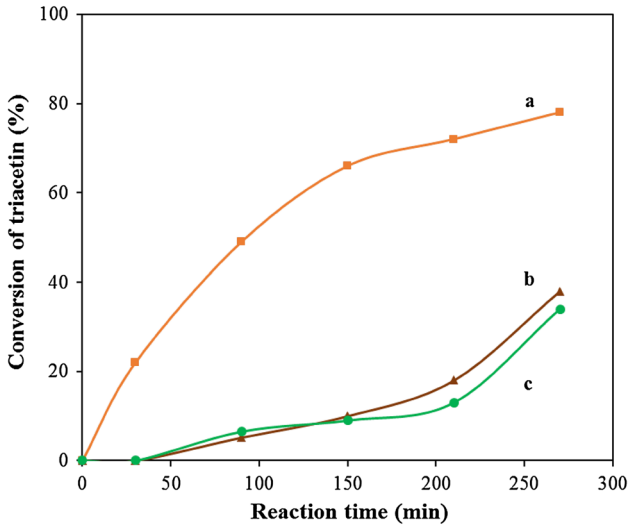

Fig. 9 Effect of reaction time on triacetin conversion over different catalysts. *a* MCM-48-NH_2 (Silica:APTES = 1:1), *b* SBA-15-NH_2 (Silica:APTES = 1:1), and *c* MCM-41-NH_2 (Silica:APTES = 1:1). Reaction conditions: catalyst 0.01 g, and temperature 65 °C

conversion plot that the catalytic performance of MCM-48-NH_2 (Silica:APTES = 1:1) is remarkably different from that of the other two catalysts, as already indicated by Fig. 8. A clear difference in activity is observed in the initial stages of the reaction. The MCM-48-NH_2 (Silica:APTES = 1:1) catalyst shows 22% conversion within 30 min. The conversion increases with time and reaches 78% after 4.5 h, whereas there is no conversion for amine-loaded MCM-41 (Silica:APTES = 1:1) and SBA-15 (Silica:APTES = 1:1) until 1.5 h. Thus, modified MCM-41 and SBA-15 are not sufficiently active in this reaction under the present optimized reaction conditions. The plot of Log Co/C vs. time (see Fig. S3, Co is the initial concentration of triacetin and C is the concentration of triacetin at different time as well as different conversion level), which confirms linear relationship between triacetin consumption and reaction time, indicating no degradation of catalytic active site during the reaction system.

3.2.3 *Effect on Amine Loading*

To gain further information concerning amine-modified MCM-48 catalyst, MCM-48 with different amine loadings was prepared. For comparison, different amine-loaded MCM-41 and SBA-15 samples were also synthesized. The amine concentration was confirmed by TG-DTA analysis. The activity of the different amine-loaded materials is summarized in Fig. 10, and shows that the conversion increases with an increase in amine concentration in all catalysts. In the case of MCM-48-NH_2, the activity increases from 12 to 78% with an increase in amine concentration from 0.17 to 1.24 mmol g^{-1}. MCM-41-NH_2 with an amine concentration of 0.38 mmol g^{-1}, and SBA-15-NH_2 with an amine concentration of 0.5 mmol g^{-1}, exhibit 4–5% triacetin conversion. Thus, even at a lower amine concentration, MCM-48-NH_2 is a superior catalyst to MCM-41-NH_2 and SBA-15-NH_2. The highest conversion is achieved with functionalized MCM-48, although the maximum amine concentration (Silica:APTES = 1:1) is slightly lower for MCM-48

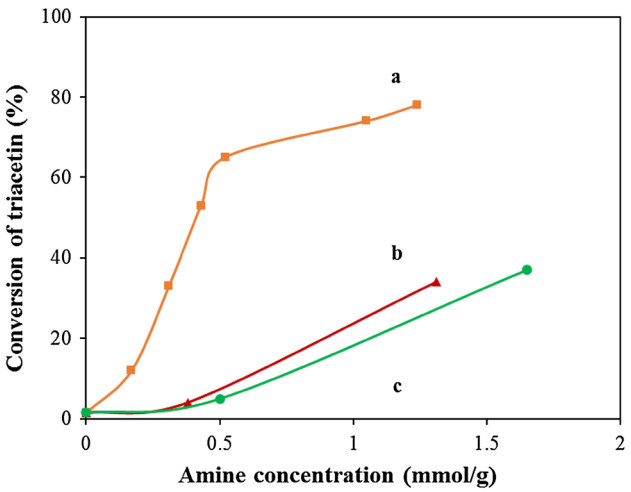

Fig. 10 Effect of amine concentration on triacetin conversion over different catalysts. *a* MCM-48-NH_2, *b* MCM-41-NH_2, and *c* SBA-15-NH_2. Reaction conditions: catalyst 0.01 g, temperature 65 °C, and time 4.5 h

(1.24 mmol g^{-1}) than MCM-41 (1.32 mmol g^{-1}) and the amine concentration is found to be maximum for SBA-15 (1.36 mmol g^{-1}).

From the results, it seems that not only the amine concentration but some other factors are responsible for the catalytic activity of the materials. The availability of the active sites clearly plays an important role in the relative catalytic activities. It was expected from the standpoints of maximum amine concentration and largest pore diameter among the mesoporous materials that SBA-15-NH_2 would be a superior catalyst to MCM-41-NH_2 or MCM-48-NH_2. Therefore, these results clearly indicate that the type of mesoporous silica is the most important factor in determining the catalytic activity of the material. The three-dimensional pore structure of MCM-48 seems to be better for site accessibility than the one-dimensional pore structures of MCM-41 and SBA-15, although the pores in SBA-15 are 2–3 times as wide as those in MCM-48.

3.2.4 *Effect of Catalyst Amount*

To get a deep insight into the catalytic system, the reaction was performed by varying the catalyst amount from 0.01 to 0.1 g (Fig. 11). Conversion was found to increase for all the catalyst with an increase in catalyst weight. When we used 0.01 g catalysts, MCM-48-NH_2 gives 48% conversion after 1.5 h, whereas MCM-41-NH_2 and SBA-15-NH_2 shows very less catalytic activity (6 and 5%). Even by using 0.1 g catalyst SBA-15-NH_2 and MCM-41-NH_2 shows around 20% triacetin conversion, the values much smaller than that on MCM-48-NH_2 (75%). This results indicate that there is

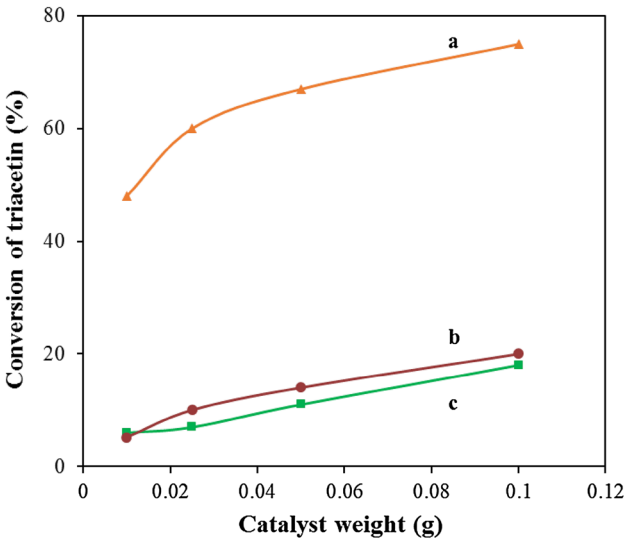

Fig. 11 Effect of catalyst amount on triacetin conversion over different catalysts. *a* MCM-48-NH_2 (Silica:APTES = 1:1), *b* MCM-41-NH_2 (Silica:APTES = 1:1), and *c* SBA-15-NH_2 (Silica:APTES = 1:1). Reaction conditions: temperature 65 °C, and time 1.5 h

diffusional limitation in this reaction system. The dimensions of triacetin is 1.02 × 0.38 nm [48]. Average pore size of MCM-48 is 2.5 nm. After amine modification the pore size remains in the range of 1.54 nm. Hence, internal diffusion of triacetin inside the pore is not a matter of concern. The turnover frequency (TOF, see Table S1) was also calculated to compare the efficiency of the catalysts based on the estimated no. of active basic site. The TOF value was found to be very high for MCM-48 catalyst than the other two at any amount of catalyst mass (0.01–0.1 g). Taking into account the fact that both MCM-48 and MCM-41 have similar surface area and amine loaded amount, the different framework structure plays important role in this reaction. We can conclude that MCM-48 with three dimensional pore structure shows high accessibility of active sites, resulting in higher catalytic efficiency.

There are several reports of the transesterification of oils over functionalized mesoporous MCM-41 and SBA-15. Liu et al. [49]. reported the transesterification of dimethyl oxalate over a series of amino-functionalized MCM-41 materials, where APTES-modified MCM-41 promoted 55% oil conversion. They used 1.8 g of catalyst, 10 h reaction time, and a reaction temperature of over 150 °C. 1-3 Dicyclohexyl-2-octylguanidine-loaded SBA-15 also showed 93% oil conversion at 65 °C [50] when the reaction was performed for 18 h and a much higher amount of catalyst was used. Thus, it is very clear that the reaction conditions used in the studies cited above were much more severe than those applied in the present study.

We attempted to optimize the reaction conditions by using the smaller amounts of catalyst and applying lower temperatures. MCM-48-NH_2 performs exceptionally well (78% triacetin conversion) at 65 °C for 4.5 h reaction time when only 10 mg of catalyst is used. However, the present mild reaction conditions were not adequate to activate MCM-41 and SBA-15 in order to explore their maximum catalytic activity. The above results indicate strongly that amine-loaded MCM-48 performs far better than MCM-41 and SBA-15 under these reaction conditions.

3.2.5 *Leaching Test*

A heterogeneity test was also performed to assess the leaching of the aminopropyl groups from the catalysts. The catalyst was filtered off from the reaction mixture after 1.5 h reaction time and the reaction was continued for another 1.5 h. A control reaction was performed for 3 h and the products of both were analyzed by GC. There is no change in the conversion of triacetin after removal of the catalyst when the reaction is continued for a further 1.5 h. Furthermore, the total conversion in this reaction after 3 h matches the conversion in the control reaction after 1.5 h. These results strongly indicate that there is no leaching of

the active species during the reaction, and that the catalyst is truly heterogeneous in nature.

3.2.6 Reusability of the Catalysts

The reusability of the catalysts was also tested. After the reaction, the catalyst was filtered, washed with methanol, and dried at room temperature. After the 1st run, the catalytic activity considerably decreases (from 78 to 34%). However, for the 2nd to 4th run, the activity remains constant. After the 2nd run, the activity remains constant, indicating that the maximum degree of deactivation is achieved during the 1st run, and that the remaining active sites are available for the next cycle of reactions. The CHN analysis reveals that after 4th cycle, the amine concentration of used catalyst is 1.08 mmol g^{-1}, which was consistent with the initial value (1.12 mmol g^{-1}). The XRD pattern (see Fig. S4) after the 4th cycle reveals that there is no structural degradation or collapse during the reactions. The FT-IR spectra (see Fig. S5) of the fresh and used catalysts also exhibit no significant difference, which is indicative of the good stability of the solid catalyst. From these results, it can be concluded that the deactivation of catalysts after 1st cycle may have occurred due to the deposition of the product or substrate within the mesopore (see TG diagram Fig. S6 where curves are compared before and after catalytic reaction).

4 Conclusion

A series of amine-modified mesoporous silica materials were prepared. Post-synthesis anchoring of organic moieties on the calcined materials was adopted, which proceeded by the condensation of silanols from a silane precursor (APTES) containing the reactive amine group. The prepared catalysts were thoroughly characterized.

The amine concentrations of the materials were calculated from TG analyses. The observed results demonstrated that the mesoporous structures of the materials were well conserved and remained unaltered even after functionalization with the aminopropyl groups.

The catalysts were tested in the transesterification of triacetin with methanol. The catalytic activity was notably different among the catalysts. MCM-48-NH_2 was found to be an efficient and environmentally benign catalyst for this reaction. Its activity was compared with those MCM-41-NH_2 and SBA-15-NH_2; and MCM-48-NH_2 showed the highest activity with 78% conversion, whereas SBA-15-NH_2 and MCM-41-NH_2 showed 37 and 34% conversion, respectively at 65 °C after 4.5 h reaction time. As the conversion of triacetin depends on basicity, the triacetin conversion increased with an increase in amine concentration. However, basicity is not the only factor upon which catalytic activity depends, and the MCM-48 materials with lower amine loadings still exhibited high catalytic activity. The results suggest that functionalized MCM-48 is a potential catalyst for this reaction and may be used for the green synthesis of biodiesel from vegetable oil, and many other industrially important liquid-phase reactions.

Acknowledgements We thank Dr. M. Maeda at the Natural Science Center for Basic Research and Development (N-BARD), Hiroshima University for the measurement of TEM measurement.

References

1. Ong YK, Bhatia S (2010) Energy 35:111–119
2. Wang S, Guo X, Wang K, Luo Z (2011) J Anal Appl Pyrolysis 91:183–189
3. Nam LTH, Vinh TQ, Loan NTT, Van Tho DS, Yang X, Su B (2011) Fuel 90:1069–1075
4. Hara M (2009) Chem Sustain Chem 2:109–135
5. Sharma YC, Singh B (2010) Biofuels Bioprod Biorefin 5:69–92
6. Serio MD, Tesser R, Pengmei L, Santacesaria E (2008) Energy Fuels 22:207–217
7. Cho YB, Seo G, Chang DR (2009) Fuel Process Technol 90:1252–1258
8. Wan T, Yu P, Gong S, Li Q, Luo Y (2008) Korean J Chem Eng 25:998–1003
9. Macleoda CS, Harvey AP, Lee AF, Wilson K (2008) Chem Eng J 135:63–70
10. Ramos MJ, Casas A, Rodriguez L, Romero R, Perez A (2008) Appl Catal A346:79–85
11. Xie W, Peng H, Chena L (2006) J Mol Catal A 246:24–32
12. Al-Zuhair S (2007) Biofuels Bioprod Biorefin 1:57–66
13. Zieba A, Drelinkaewicz A, Chmielarz P, Matachowski L, Stejskal J(2010) Appl Catal A 387:13–25
14. Zhang Y, Wong W-T, Yung K-F (2014) Appl Energy 116:191–198
15. Barot S, Nawab M, Bandyopadhyay R (2016) J Porous Mater 23:1197–1205
16. Suppes GJ, Dasari MA, Doskocil EJ, Mankidy PJ, Goff MJ (2004) Appl Catal A 257:213–223
17. Lopez DE, Goodwin JG Jr, Bruce DA, Lotero E (2005) Appl Catal A 295:97–105
18. Kresge CT, Leonowicz ME, Roth WJ, Vartuli JC, Beck JS (1992) Nature 359:710–712
19. Corma A (1997) Chem Rev 97:2373–2419
20. Feng X, Frixell GE, Wang LQ, Kim AY, Liu J, Kemner KM (1997) Science 276:923–926
21. Liu AM, Hidajat K, Kawi S, Zhao DY (2000) Chem Commun 13:1145–1146
22. Hata H, Saeki S, Kimura T, Sugahara Y, Kuroda K (1999) Chem Mater 11:1110–1119
23. Zhao D, Yang P, Huo Q, Chmelka BF, Stucky GD (1998) Curr Opin Solid State Mater Sci 3:111–121
24. Yokoi T, Yoshitake H, Tatsumi T (2004) J Mater Chem 14:951–957
25. Xia YD, Wang WX, Mokaya R (2005) J Am Chem Soc 127:790–798
26. Yang Q, Liu J, Yang J, Zhang L, Feng Z, Zhang J, Li C (2005) Microporous Mesoporous Mater 77:257–264
27. Zeng X, Qian X-F, Win J, Zhu Zi-K (2006) Mater Chem Phys 97:437–444

28. Wei Q, Chen H-Q, Nie Z-R, Hao Y-L, Wang Y-L, Li Q-Y, Zou J-X (2007) Mater Lett 61:1469–1473
29. Knofel C, Descarpentries J, Benzaouia A, Zelenak V, Mornet S, Llewellyn PL, Hornebecq V (2007) Microporous Mesoporous Mater 99:79–85
30. Manzano M, Aina V, Arean CO, Balas F, Cauda V, Colilla M, Delgado MR, Regi MV (2008) Chem Eng J 137:30–37
31. Bandyopadhyay M, Shiju NR, Brown DR (2010) Catal Commun 11:660–664
32. Melendez-Ortiz HI, Perera-Marcado YA, Mercado-Silva JA, Maldonado YO, Castruita G, Garcia-Cerda LA (2014) Ceramic Int 40:9701–9707
33. de Lima AL, Mbengue A, San Gil RAS, Ronconi CM, Mota CJA (2014) Catal Today 226:210–216
34. Hu G, Li P, Feng H, Zhang X, Chu PK (2015) J Mater Chem B 10:2024–2042
35. de Leon GC, Perea-Mercado YA, Garcia-Cerda LA, Mercado-Silva JA, Melendez-Ortiz HI, Maldonado YO, Contreras LA (2015) Microporous Mesoporous Mater 204:156–162
36. Cheah WK, Sim Y-L, Yeoh F-Y (2016) Mater Chem Phys 175:151–157
37. Meziani MJ, Zajac J, Jones DJ, Patyka S, Roziere J, Auroux A (2000) Langmuir 16:2262–2266
38. Brunel D, Blanc A C, Galarneau A, Fajula F (2002) Catal Today 73:139–152
39. Guerrero VV, Shantz DF (2009) Ind Eng Chem Res 48:10375–10380
40. Gies H, Grabowski S, Bandyopadhyay M, Grunert W, Tkachenko OP, Klementiev KV, Birkner A (2003) Microporous Mesoporous Mater 60:31–42
41. Lesaint C, Lebeau B, Marichal C, Patarin J (2005) Microporous Mesoporous Mater 83:76–84
42. Wang X, Tseng Y-H, Chan JCC, Cheng S (2005) Microporous Mesoporous Mater 85:241–251
43. Tsunoji N, Takahashi K, Sadakane M, Sano T (2014) Bull Chem Soc Jpn 87:1379–1385
44. Yoshitake H, Yokoi T, Tatsumi T (2002) Chem Mater 14:4603–4610
45. Li Y, Zhou G, Li C, Qin D, Qiao W, Chu B (2009) Colloids Surf A 341:79–85
46. Yoshitake H, Yokoi T, Tatsumi T (2004) Chem Mater 14:951–957
47. Konwar LJ, Arvela PM, Begam P, Kumar N, Thakur AJ, Mikkola PJ, Deka RC, Deka D (2015) J Catal 329:237–247
48. Silveira JQ, Vargas MD, Ronconi CM (2011) J Mater Chem 21:6034–6039
49. Liu Y, Zhao G, Zhu W, Wang J, Liu G, Zhang W, Jia M (2010) J Braz Chem Soc 21:2254–2261
50. Zie W, Yang X, Fan M (2015) Renew Energy 80:230–237